

1002  
1N-90  
324458

# Computer Modeling of the Thermal Conductivity of Cometary Ice: Final Report for Contract# NCC2-5147

Theodore E. Bunch, Michael A. Wilson, and Andrew Pohorille,  
Exobiology Branch, NASA Ames Research Center,  
Moffett Field, CA 94035

July 14, 1998

## Objectives

The main objective of this research project was to estimate the thermal conductivity of cometary ices from computer simulations of model amorphous ices. This was divided into four specific tasks:

1. Generating of samples of amorphous water ices at different microporosities;
2. Comparing the resulting molecular structures of the ices with experimental results, for those densities where data was available;
3. Calculating the thermal conductivities of liquid water and bulk amorphous ices and comparing these results with experimentally determined thermal conductivities;
4. Investigating how the thermal conductivity of amorphous ice depends upon the microscopic porosity of the samples.

## Summary

The thermal conductivity was found to be only weakly dependent on the microstructure of the amorphous ice. In general, the amorphous ices were found to have thermal conductivities of the same order of magnitude as liquid water. This is in contradiction to recent experimental estimates of the thermal conductivity of amorphous ice, and it is suggested that the extremely low value obtained experimentally is due to larger-scale defects in the ice, such as cracks, but is not an intrinsic property of the bulk amorphous ice.

**Period of Performance:** September 1, 1995 – April 30, 1998

**Inventions:** There are no patents or inventions arising from this research project.

## Introduction

It is thought that the ices in the region outside the solar system are representative of the protostellar nebula from which the solar system was formed (Klinger, 1983). Comets and interstellar dust grains are thought to reflect the composition of the protostellar nebula, having existed in an unaltered state since the formation of the solar system. It is also thought that much of the water and biogenic material on the earth was delivered by cometary impacts after the initial formation of the planets. Thus, understanding the physical and chemical state of the icy interior of cometary bodies would provide not only a more detailed understanding of the early solar system, but would also yield information on the form and composition of biogenic elements as they were introduced to the earth (Chyba *et al.*, 1990).

A great deal has been learned about astrophysical ices through infrared astronomical observation of interstellar molecular clouds, planets, icy satellites and cometary bodies (Hagen *et al.*, 1979; Sandford and Allamandola, 1990b; Sandford and Allamandola, 1990a; Cruikshank *et al.*, 1993; Owen *et al.*, 1993; Irvine *et al.*, 1996). Our understanding of astrophysical ices has been aided by ground-based experiments (Hallbrucker *et al.*, 1991; Klug *et al.*, 1991; Jenniskens and Blake, 1994; Devlin and Buch, 1995) and computational studies (Zhang and Buch, 1990a; Zhang and Buch, 1990b; Buch, 1990; Buch, 1992; Wilson *et al.*, 1995; Essmann and Geiger, 1995). Computational studies are particularly well suited for investigating conditions which cannot be obtained in the laboratory, such as the formation of cold (10–15 K) amorphous ice from cold water vapor.

Cometary bodies which pass near the sun, however, are subject to solar radiation, giving rise to possible structural changes in the icy mantle as well as out gassing of volatile constituents (Priolnik and Barnun, 1990; Notesco *et al.*, 1991; Notesco and Bar-Nun, 1997). The extent to which this processing occurs depends upon the thermal conductivity of the amorphous ice. In addition to its importance in cometary evolution, the thermal conductivity is also important in the formation of ice on interstellar dust grains. Recent experiments have led to widely different values of the thermal conductivity, and the problem has not been resolved (Kouchi *et al.*, 1992).

## Methods

In an MD simulation, the equations of motion of the system are solved numerically, and the properties of interest are obtained from averages over the resulting numerical trajectories. The majority of MD calculations are based on classical mechanical models, and the problem reduces to the solution of Newton's equations of motion for a system of interacting atoms and/or molecules. A detailed descriptions of this method can be found in a number of basic texts (Allen and Tildesley, 1987; Hansen and McDonald, 1986).

Several models are available to describe the interactions between water molecules. We have selected the TIP4P model (Jorgensen *et al.*, 1983) which has been shown to provide a good description of liquid water, as found through the comparison of the water–water pair correlation functions with the results of neutron scattering experiments (Jorgensen *et al.*, 1983), as well as the liquid–vapor interface of water (Wilson *et al.*, 1987). The TIP4P model can also reproduce many physical properties of crystalline ices (Tse and Klein, 1988a), and the pressure disordered high and low density amorphous ices (Tse and Klein, 1988b). Related studies on solid amorphous ice phases have been done using the ST2 model of water (Poole

*et al.*, 1992), and amorphous ice clusters using the TIPS2 model (Zhang and Buch, 1990a; Zhang and Buch, 1990b; Buch, 1990; Buch, 1992).

The methodology for generating these structures has been described previously (Wilson *et al.*, 1995). Briefly, the TIP4P model of water was used throughout the simulations (Jorgensen *et al.*, 1983), which has been shown to reproduce correctly many of the structural properties of water and aqueous solutions. 343 water molecules were placed in a cubic box at a density of 0.94 g/cc for the lda ice and 1.17 g/cc for the hda ice. The systems were simulated at a temperature of 300 K for 1.1 ns. Configurations were stored every 10 ps over the final 1.0 ns of the run. At 300 K, the correlation time for water is less than 10 ps, so this yields a set of 100 uncorrelated configurations at each density, for a total of 200 configurations. It is important to start with an uncorrelated set of configurations: At the temperatures of interest, 10-77 K, a trajectory started from a single configuration will undergo very few structural rearrangements on the time scale that can be followed in a computer simulation. Constructing averages over a set of uncorrelated configurations avoids this “initial conditions” problem. Each of the 200 configurations was slowly annealed to 10 K by cooling the configuration in 50 K increments over 50 ps followed by a constant temperature trajectory of 50 ps.

## Results

### Bulk Amorphous Ices

We have carried out computer simulations of bulk amorphous ices at the densities of the two major polymorphs: 0.94 g/cc for low density amorphous (lda) ice and 1.17 g/cc for the high density amorphous (hda) ice (Narten *et al.*, 1976). The structure of the ices, as determined from the pair-correlation functions, was found to be in good agreement with the correlation functions obtained from neutron scattering experiments. This demonstrates that the water models used in our computer simulations provide a good description of the bulk amorphous ice phases. The neutron-weighted structure factors,  $G(r)$ , of the low and high density ices computed from the bulk quenches are shown in Figure 1. These are in good agreement with experimentally determined structure factors (not shown) (Bellissent-Funel *et al.*, 1987). The neutron-weighted pair correlation function,  $G(r)$ , is related to the usual atom-atom radial distribution functions by  $G(r) = 4\pi\rho r \times (0.092G_{O-O}(r) + 0.422G_{O-H}(r) + 0.486G_{H-H}(r) - 1)$  where the numerical coefficients are scattering weights associated with the neutron scattering experiments.

Detailed information about the nature of the hydrogen-bonding network of the ices can be obtained from the oxygen-oxygen radial distribution functions (RDF's), shown in Figure 2. The oxygen-oxygen RDF of lda ice is similar to that of liquid water, also shown in Figure 2. The location of the first and second peaks at 2.75 Å and 4.45 Å in the RDF are indicative of the tetrahedral ordering found in liquid water. This result is in good agreement with X-ray diffraction results on pressure induced lda ice (not shown) (Bizid *et al.*, 1987). The main difference between the computer simulation results and the X-ray data is that the first peak is much broader in the X-ray data, which suggests that the computer simulated ices may not be fully relaxed.

In contrast, the first peak in the oxygen-oxygen RDF of hda ice is smaller and broader than for lda ice, and the second peak is very broad and shifted to smaller distances, indicating a greatly distorted hydrogen bond network. The X-ray results on hda ice also show

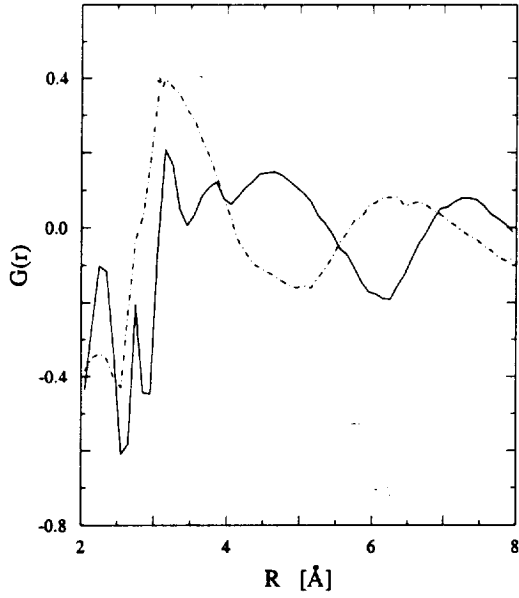


Figure 1: Neutron-weighted scattering functions from computer simulations of lda (solid line) and hda (dot-dashed line) ice.

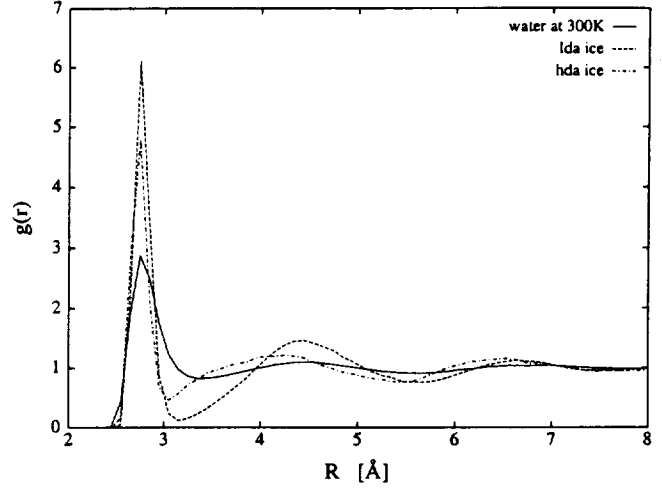


Figure 2: Oxygen-oxygen pair correlation functions for water at 300 K, lda ice and hda ice.

substantially less structure than the lda ice. However, the agreement between the RDF of the computer simulated hda ice and the X-ray diffraction results (Bizid *et al.*, 1987) is only qualitative. In particular, the X-ray RDF of the hda ice exhibits two next-nearest neighbor peaks at 3.7 Å and 4.65 Å, of which the 3.7 Å is due to the presence of water triplets with small O-O-O angles. This feature appears to be absent in simulated hda ice, although it is possible that the single broad peak observed here, which spans the region from 3.7 Å to 4.7 Å, is not completely relaxed, and would split into two peaks with additional annealing.

These results demonstrate that the TIP4P model adequately represents the structural properties of bulk samples of the hda and lda ices. The bulk lda and hda samples were then used as the initial substrates in simulations to generate samples at different microporosities.

### Calculation of the Thermal Conductivity of Amorphous Ice

The thermal conductivity,  $\kappa$ , can be calculated from the long-time limit of the heat flux correlation function,

$$\kappa = \frac{1}{2k_B VT^2} \lim_{t \rightarrow \infty} \frac{d}{dt} \left\langle \sum_{i,j=1}^N E_i(t) E_j(0) (x_i(t) - x_i(0))^2 \right\rangle,$$

where  $k_B$  is the Boltzmann constant,  $T$  and  $V$  are the temperature and volume of the system, respectively, and  $E_i(t)$  and  $x_i(t)$  are the energies and positions of molecule  $i$  at time  $t$ . The double sum is over all  $N$  molecules in the system, and  $\langle \dots \rangle$  denotes a statistical average.

The heat flux correlation for liquid water is shown in Figure 3. The thermal conductivity of water is determined from the slopes of these curves in the long-time, linear regime. It is

found to be 0.19, 0.23 and 0.26  $\text{W}\cdot\text{m}^{-1}\cdot\text{K}^{-1}$  for temperatures of 290, 300 and 310 K, respectively. These values are between 2 and 3 times lower than the experimentally determined thermal conductivities of water at the same temperatures: 0.5917, 0.6096 and 0.6252  $\text{W}\cdot\text{m}^{-1}\cdot\text{K}^{-1}$ . While this difference is fairly large, it is small compared to the differences between the measured thermal conductivity of water and experimental estimates of the thermal conductivity of amorphous ice. Thus, our computer simulations provide a sufficiently accurate description of the thermal transport properties of water that meaningful conclusions can be drawn from subsequent calculations of the thermal conductivity of the amorphous ice as a function of the degree of its microporosity.

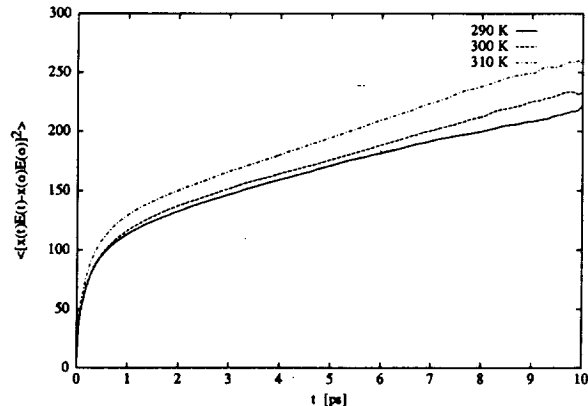


Figure 3: Heat flux current correlation function for bulk liquid water at 290 K, 300 K and 310 K.

to investigate the possible extremes of the microporous structures: random deletion of water molecules results in a fairly uniform distribution of small cavities in the structure whereas deleting around a fixed center yields much larger cavities.

The heat flux correlation function for the two microporous samples of amorphous ice are shown in Figure 4. These are qualitatively similar to the results for liquid water, shown in Figure 3, in particular, both the liquid and amorphous samples reach the linear regime on the same time scales and the curves have slopes that are of the same order of magnitude. The main difference between the liquid and amorphous figures is that the heat flux correlation of for the amorphous substrates makes a more abrupt transition to the linear regime. This is due to the lack of relaxation in the energy flux via mass transport in the amorphous ice samples over the time scales of the computer simulation. What is most significant is that the results of random deletion of water molecules, giving rise to a large number of smaller micropores, is not qualitatively different than the results for deletion of

To create samples of microporous amorphous ice, we carried out high temperature simulations at 300 K with fixed bulk densities of 0.9, 0.8 and 0.7 g/cc. Configurations from these calculations were quenched to 77 K to provided a set of initial conditions for calculations of the thermal conductivity. To investigate how different microporous structures might affect the thermal conductivity, we devised two methods for generating such structures. In the first method, we took a set of 1da ice configurations and randomly deleted water molecules until the density was 0.7 g/cc. The second procedure was to delete water molecules around a fixed center until a density of 0.7 g/cc was reached. This allows us

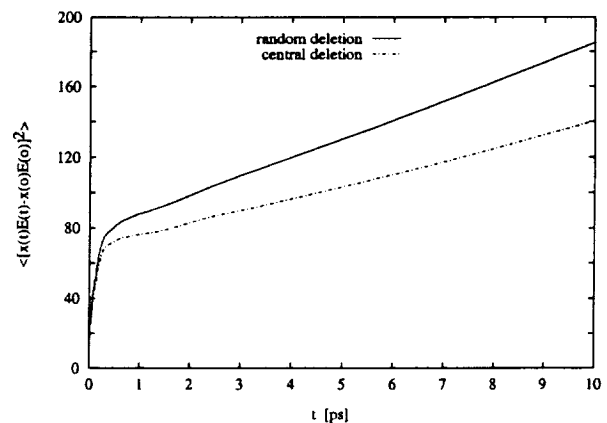


Figure 4: Heat flux current correlation for microporous amorphous ices at 0.7 g/cc.

**Thermal Conductivities of Water and Amorphous Ices**

	T(K)	MD $\kappa$ (W-m <sup>-1</sup> -K <sup>-1</sup> )	exptl
Water	290	0.19±0.02	0.5917 <sup>a</sup>
	300	0.23±0.02	0.6096 <sup>a</sup>
	310	0.26±0.01	0.6252 <sup>a</sup>
Ice Ih <sup>b</sup>	100	1.49	5.94
	260	0.94	2.35
LDA	93	0.15	4×10 <sup>-5</sup> (80-100 K) <sup>c</sup>
HDA	93	0.35	
microporous <sup>d</sup>			
0.9 g/cc	86	0.12±0.02	
0.8 g/cc	85	0.10±0.02	
0.7 g/cc	86	0.10, 0.23 <sup>e</sup> (87 K), 0.14 <sup>f</sup> (92 K)	

<sup>a</sup>Ramires, *et al.*, J. Phys. Chem. Ref. Data (1995) **24**, 1377-1381.

<sup>b</sup>Ice Ih results are from: Inoue, *et al.*, J. Chem. Phys. (1996) **102**, 9569-9577.

<sup>c</sup>Kouchi, *et al.*, Astrophysical J. **388**, L73-L76.

<sup>d</sup>micropores created by annealing at fixed density from liquid.

<sup>e</sup>micropores created by random deletion of water molecules followed by quenching.

<sup>f</sup>micropores created by deletion around a fixed center followed by quenching.

water molecules around a single center, creating a single, large void in the sample. Consequently, even at the low density of 0.7 g/cc, we find no evidence for a greatly reduced thermal conductivity in either extreme of a few, large micropores or uniformly dispersed micropores.

The computed thermal conductivities of the various water and amorphous ice runs simulations are summarized in Table 1, as well as the computed thermal conductivities of the hda and lda ice. They are of the same order of magnitude as the results for liquid water. This result is reasonable because the structure of amorphous ice is quite similar to liquid water. The thermal conductivity of crystalline ice Ih at 100 K is 5.95 W-m<sup>-1</sup>-K<sup>-1</sup>, over an order of magnitude larger than the thermal conductivity of amorphous ice at similar temperatures.

The main result is that the thermal conductivity of the microporous ices appear to be of the same order of magnitude as the bulk amorphous ices. The thermal conductivity does not decrease dramatically as the density of the amorphous ice is reduced from 0.94 g/cc to 0.7 g/cc. Since the thermal conductivities for ice samples containing large cavities and uniformly distributed small cavities differ by only a factor of 2 we conclude that the bulk thermal conductivity is not very sensitive to the distribution of the micropores. Therefore, the microporosity of the ice does not explain the extremely low value of thermal conductivity that has been reported for vapor deposited amorphous ice.

## Significance

Since all hypotheses about the role of comets in the origin of life and chemical evolution of the solar system make explicit or implicit assumptions about the thermal conductivity of

the cometary ice, the results of our calculations provide crucial information for the critical evaluation of these hypotheses. Recent experiments on laboratory analogs of cometary ice have yielded values of the thermal conductivity that are several orders of magnitude lower than the thermal conductivity of bulk amorphous ices. If this is true, then it implies that the interiors of comets are not heated at the perihelion of their orbits. Consequently, the interiors of comets might not have undergone any significant amount of thermal processing and their composition might reflect the composition of the protostellar nebula.

Whereas the laboratory analogs of cometary ice are prepared by slowly depositing water vapor onto a cold substrate, the bulk amorphous ices are prepared by applying extreme pressure to crystalline ice samples until the underlying lattice is disrupted. It was originally thought that the low measured value of the thermal conductivity might be due to the microscopic porosity of the ice sample. As the computed thermal conductivities of several samples of microporous ice do not appear to be extremely sensitive to the microscale structure of the ice, we conclude that an extremely low thermal conductivity is not a property of amorphous ice, even at densities as low as 0.7 g/cc considering several extremes of how the microscale structure of the ice is induced. Rather, our results indicate that the thermal conductivity of microporous, amorphous ice samples are similar to bulk amorphous ices. Consequently, it is likely that the thermal conductivity of astrophysical ice is of the same order of magnitude as normal ice.

It is possible that the extremely low thermal conductivity measured in the vapor deposition experiments is due to larger scale defects, such as cracks. In this case, the macroscopic thermal conductivity is determined by the heat flux across such defects and not the bulk thermal conductivity of the bulk amorphous ice. In the laboratory, the initial density of the ice will depend upon a number of factors including the deposition rates and the temperature of the substrate (Jenniskens and Blake, 1994), and amorphous ice layers from smooth and dense (Jenniskens and Blake, 1994) to extremely porous and “fluffy” (Laufer *et al.*, 1987) can be obtained with different initial conditions.

**Publications:** “The Thermal Conductivity of Cometary Ice”, M. A. Wilson, and A. Pohorille, (to be published, 1998).

**Keywords:** thermal conductivity, microporosity, amorphous ice, cometary ices

## References

- Allen, M.P., and Tildesley, D.J. (1987). "Computer Simulation of Liquids." Clarendon Press, Oxford.
- Bellissent-Funel, M.-C., Teixeira, J., and Bosio, L. (1987). *J. Chem. Phys.* **87**, 2231–2235.
- Bizid, A., Bosio, L., Defrain, A., and Oumezzine, M. (1987). *J. Chem. Phys.* **87**, 2225–2230.
- Buch, V. (1990). *J. Chem. Phys.* **93**, 2631–2639.
- Buch, V. (1992). *J. Chem. Phys.* **96**, 3814–3823.
- Chyba, C.F., Thomas, P.J., Brookshaw, L., and Sagan, C. (1990). *Science* **249**, 366–373.
- Cruikshank, D.P., Roush, T.L., Owen, T.C., Geballe, T.R., deBergh, C., Schmitt, B., Brown, R.H., and Bartholomew, M.J. (1993). *Science* **261**, 742–745.
- Devlin, J.P., and Buch, V. (1995). *J. Phys. Chem.* **99**, 16534–16548.
- Essmann, U., and Geiger, A. (1995). *J. Chem. Phys.* **103**, 4678–4692.
- Hagen, W., Allamandola, L.J., and Greenberg, J.M. (1979). *Astrophys. Space Sci.* **65**, 215–.
- Hallbrucker, A., Mayer, E., O'Mard, L.P., Dore, J.C., and Chieux, P. (1991). *Phys. Lett. A* **159**, 406–410.
- Hansen, J.P., and McDonald, I.R. (1986). "Theory of Simple Liquids." Academic Press, New York.
- Irvine, W.M., Bockelée-Morvan, D., Lis, D.C., Matthews, H.E., Biver, N., Crovisier, J., Davies, J.K., Dent, W.R.F., Gautier, D., Godfrey, P.D., Keene, J., Lovell, A.J., Owen, T.C., Phillips, T.B., Rauer, H., Schloerb, F.P., Senay, M., and Young, K. (1996). *Nature* **383**, 418–428.
- Jenniskens, P., and Blake, D.F. (1994). *Science* **265**, 753–756.
- Jorgensen, W.L., Chandrasekhar, J., Madura, J.D., Impey, R.W., and Klein, M.L. (1983). *J. Chem. Phys.* **79**, 926–935.
- Klinger, J. (1983). *J. Phys. Chem.* **87**, 4209–4214.
- Klug, D.D., Whalley, E., Svensson, E.C., Root, J.H., and Sears, V.F. (1991). *Phys. Rev. B* **44**, 841–844.
- Kouchi, A., Greenberg, J.M., Yamamoto, T., and Mukai, T. (1992). *Astrophys. J.* **388**, L73–L76.
- Laufer, D., Kochavi, E., and Bar-Nun, A. (1987). *Phys. Rev. B* **36**, 9219–9227.
- Narten, A.H., Venkatesh, C.G., and Rice, S.A. (1976). *J. Chem. Phys.* **64**, 1106–1121.



- Notesco, G., and Bar-Nun, A. (1997). *Icarus* **126**, 336–341.
- Notesco, G., Kleinfeld, I., Laufer, D., and Bar-Nun, A. (1991). *Icarus* **89**, 411–413.
- Owen, T.C., Roush, T.L., Cruikshank, D.P., Elliot, J.L., Young, L.A., deBergh, C., Schmitt, B., Geballe, T.R., Brown, R.H., and Bartholomew, M.J. (1993). *Science* **261**, 745–748.
- Poole, P.H., Sciortino, F., Essmann, U., and Stanley, H.E. (1992). *Nature* **360**, 324–328.
- Prialnik, D., and Barnun, A. (1990). *Astrophys. J.* **363**, 274–282.
- Sandford, S.A., and Allamandola, L.J. (1990a). *Astrophys. J.* **355**, 357–372.
- Sandford, S.A., and Allamandola, L.J. (1990b). *Icarus* **87**, 188–192.
- Tse, J.S., and Klein, M.L. (1988a). *J. Phys. Chem.* **92**, 315–318.
- Tse, J.S., and Klein, M.L. (1988b). *J. Chem. Phys.* **92**, 3992–3994.
- Wilson, M.A., Pohorille, A., and Pratt, L.R. (1987). *J. Phys. Chem.* **91**, 4873–4878.
- Wilson, M.A., Pohorille, A., Jenniskens, P., and Blake, D.F. (1995). *Origins Life Evol. Biosphere* **25**, 3–19.
- Zhang, Q., and Buch, V. (1990a). *J. Chem. Phys.* **92**, 5004–5016.
- Zhang, Q., and Buch, V. (1990b). *J. Chem. Phys.* **92**, 1512–1513.